Highlights on Spanish Astrophysics X, Proceedings of the XIII Scientific Meeting of the Spanish Astronomical Society held on July 16 – 20, 2018, in Salamanca, Spain. B. Montesinos, A. Asensio Ramos, F. Buitrago, R. Schödel, E. Villaver, S. Pérez-Hoyos, I. Ordóñez-Etxeberria (eds.), 2019

Deep imaging of the most massive galaxies of the nearby Universe.

S. N. dos Reis[1,2], F. Buitrago[1,2], and P. Papaderos[3]

[1] Instituto de Astrofísica e Ciências do Espaço, Universidade de Lisboa, OAL, Tapada da Ajuda, PT1349-018 Lisboa, Portugal
[2] Departamento de Física, Faculdade de Ciências da Universidade de Lisboa, Edifício C8, Campo Grande, PT1749-016 Lisboa, Portugal
[3] Instituto de Astrofísica e Ciências do Espaço, Universidade do Porto, CAUP, Rua das Estrelas, PT4150-762 Porto, Portugal

Abstract

Taking advantage of deep photometric data from HST, we analyze the $z < 0.5$ massive galaxies obtained in the H- and I-bands, in order to disentangle the several components that might constitute most massive galaxies in our Universe. We perform single and double-Sérsic analysis for our sample of 17 galaxies. From our photometric analysis, we notice that Sérsic index values are not a good representation of a galaxy' morphological type and find no trend between B/T and redshift. We detect within our sample two late-type galaxies with sizes smaller than expected. Additionally, our set of simulations shows that the apparent magnitudes and Sérsic index are the key parameters to a good recovery of the structural parameters.

1 Introduction

The most massive ($M_{\mathrm{stellar}} \geq 10^{11} M_{\odot}$) galaxies in the Universe undergo a dramatic transformation in their observational properties across cosmic time, from compact star-forming disks to huge red and dead spheroidal galaxies [3]. However, how galaxies acquire their mass and how they evolve morphologically are still open questions. One important finding from the work by [3] is that late-type galaxies (LTGs) and irregular objects are the dominant morphologies among massive galaxies at $z \sim 2.5$, whereas since $z \sim 1$ they are dominated generally by early-type galaxies (ETGs).

The current most favored galaxy formation model for massive galaxies is a two-phase formation scenario that predicts a rapid formation phase at $2 < z < 6$ dominated by in-situ star formation [12], and a second phase in which they are predicted to suffer intense minor mergers [8, 9, 11, 2, 10, 5, 4] that may transform them into the spheroids that we see today.

The availability of deep photometric data from the Hubble Space Telescope (HST) with combination of 3D-spectroscopy surveys allows a detailed analysis of these massive systems to investigate their structure and evolution. The part dedicated to the deep photometric data is presented here, and it is by means of multi-band surface photometry and bulge-disk profile decompositions of 17 nearby ($z < 0.5$) massive galaxies from the Cosmic Assembly Near-infrared Deep Extragalactic Legacy Survey (CANDELS)[1] [6, 7].

2 Analysis

For our analysis we used two filters: F160W (WFC3 H-band) which is the reddest HST filter, and F814W (ACS I-band) corresponding to the closest to the optical rest-frame.

We used SExtractor [1] to identify the neighboring objects to be masked or chosen to be fit simultaneously with the galaxy target. The values of apparent magnitude, size, axis ratio and position angle retrieved from SExtractor were then used as initial guesses in fitting the galaxies' structural parameters with GALFIT [13]. We performed single Sérsic fits and bulge-disk decompositions with the aim to describe each galaxy's surface brightness profile as accurately as possible, and to disentangle between a bulge and a disk in the case of a LTG, or to check if an ETG is purely elliptical or contains other components (e.g., a disk or bar).

After a detailed analysis trying to retrieve the best possible fit to our galaxy sample, we derived their sizes. Following the definition of effective radius (r_e), we computed curves of growth for the best-fitting two-component GALFIT models by integrating the flux within concentric elliptical apertures until we reach half of the galaxy total flux. These multi-component r_e are expected to yield a more accurate measure of size since the two-component fits generally provide a better match to the 2D surface brightness distribution of our sample galaxies than a single Sérsic model.

We further derived the surface brightness profiles for each galaxy and construct a mass-size relation for the sake of comparison with standard references in the literature.

Additionally, we conducted a set of simulations to test the robustness of our measured structural parameters, both for the H- and I-bands. This was achieved by creating $\sim$2500 mock galaxies uniformly distributed along the entire parameter space value ranges of the structural parameters from our analysis, placing each galaxy randomly on the correspondent band image and convolving with the respective PSF. We analyzed each artificial galaxy with the same methodology used in our real sample for the single Sérsic fits.

3 Results

Figure 1 shows the histograms obtained for the two bands' single Sérsic fits. Following [14] who use $n = 2.5$ as a division line between ETGs and LTGs, our sample would result in two

[1] `http://candels.ucolick.org/data_access/Latest_Release.html`

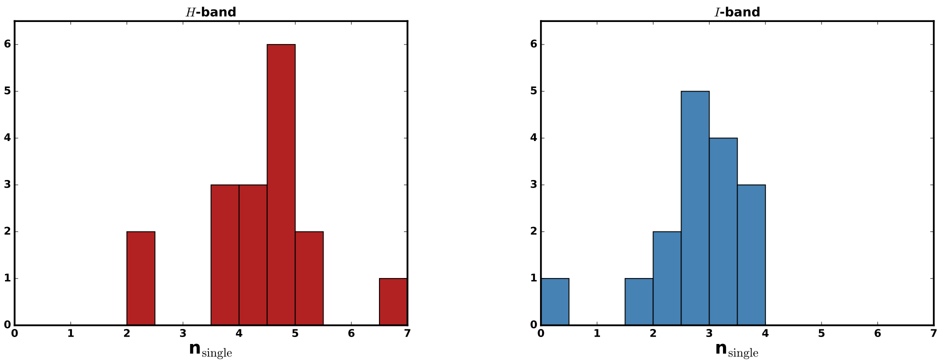

Figure 1: Sérsic index histograms for single-Sérsic fits values, both for the H-band (left) and the I-band (right). It is remarkable that in the H-band our sample contains nine visually classified LTGs, yet accordingly with Sérsic index fits only two would be classified as disk-like objects ($n < 2.5$).

galaxies classified as disk-like ($n < 2.5$) in the H-band, and four in the I-band, but by visual inspection in the H-band we classified nine galaxies as being LTGs. Our results imply that the Sérsic index provides a poor means for the quantification of the visual morphology of our galaxy population.

We construct the mass-size relation for our H-band data in Fig. 2 and compare with the results from [14] and from [16] for the lowest redshift bin centered at $z = 0.25$. ETGs are represented with red dotted points and the LTGs with spiral points (blue or purple in the case of a galaxy with a bar). We show in the y-axis the computed multi-component effective radii. The results from [16] for each galaxy in our sample, which were inferred from fitting single Sérsic functions, are represented by a triangle and connected with a line to our data. The colored dashed lines correspond to [16] at $z = 0.25$ (red for ETGs and blue for LTGs), while the red and blue shaded regions correspond to [14] local relation. Our results are consistent with those found by [14], having almost the entire sample falling inside their scatter. There are however two LTGs with sizes $\sim 2\sigma$ under the relation, being then much smaller than expected. These objects are worth a further investigation in the future.

In Fig. 3 we present surface brightness profiles for two representative galaxies from our sample that were visually classified as being ETG (top panels) and LTG with a bar (bottom panels). The left panels show the profiles in the H-band whereas the right panels in the I-band. Inside each profile we display the corresponding galaxy stamp in units of surface brightness (mag arcsec^{-2}) with shadowed areas matching the masks used to recover the observed light profile. All galaxies in our sample are more luminous in the H-band. For most of the objects in our sample we obtain an over-prediction of the light in the outskirts when performing a single-Sérsic fit (solid purple line). By using more Sérsic functions we recover a better description of the total light distribution, thus having a better match between the observed profile (black points) and the multi-component fit (solid green line). Nevertheless, for most of the cases, the light is under-estimated in the outskirts of our multi-component

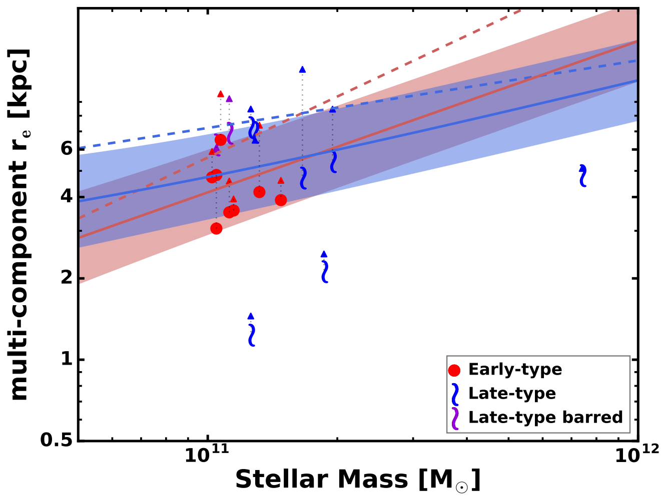

Figure 2: Size-stellar mass distribution of our H-band data, linked to [16] results represented by a triangle. The colored dashed lines correspond to [16] at $z = 0.25$. [14] local relation for ETGs and LTGs is represented by the solid red and blue lines, respectively, with the corresponded scatter being the shaded red and blue regions. Our results are in agreement with [14], having most of our sample matching the local relation. However, there are two LTGs smaller than expected (by $\sim 2\sigma$), thus being interesting to further investigate.

Sérsic fits.

Our set of simulations on mock galaxy images demonstrates that, on the statistical average, GALFIT can retrieve Sérsic model parameters with a satisfactory accuracy. However individual fits can yield substantial systematic deviations from observed profiles, in particular in their low-surface brightness periphery. Uncertainties in non-linear fitting and also the mathematical nature of the Sérsic law itself can be the ones to blame for such deviations.

The strong dependence of the fit on the central data points urges for a precise correction for PSF convolution effects and offers an explanation for systematic deviations between the best-fitting Sérsic model and the observed SBP in the low-surface brightness periphery of galaxies. From several GALFIT models from our sample, both single and multi-component fits, such deviations are apparent at the level of ~ 1, requesting for a careful judgment of solutions from GALFIT and parametric image decomposition tools in general. A conclusive investigation of the buildup history of the extended stellar envelope of massive galaxies appeals for a test in whether the color profiles implied by subtraction of GALFIT models in two different bands are replicatable by evolutionary synthesis models and consistent with a two-phase galaxy formation scenario.

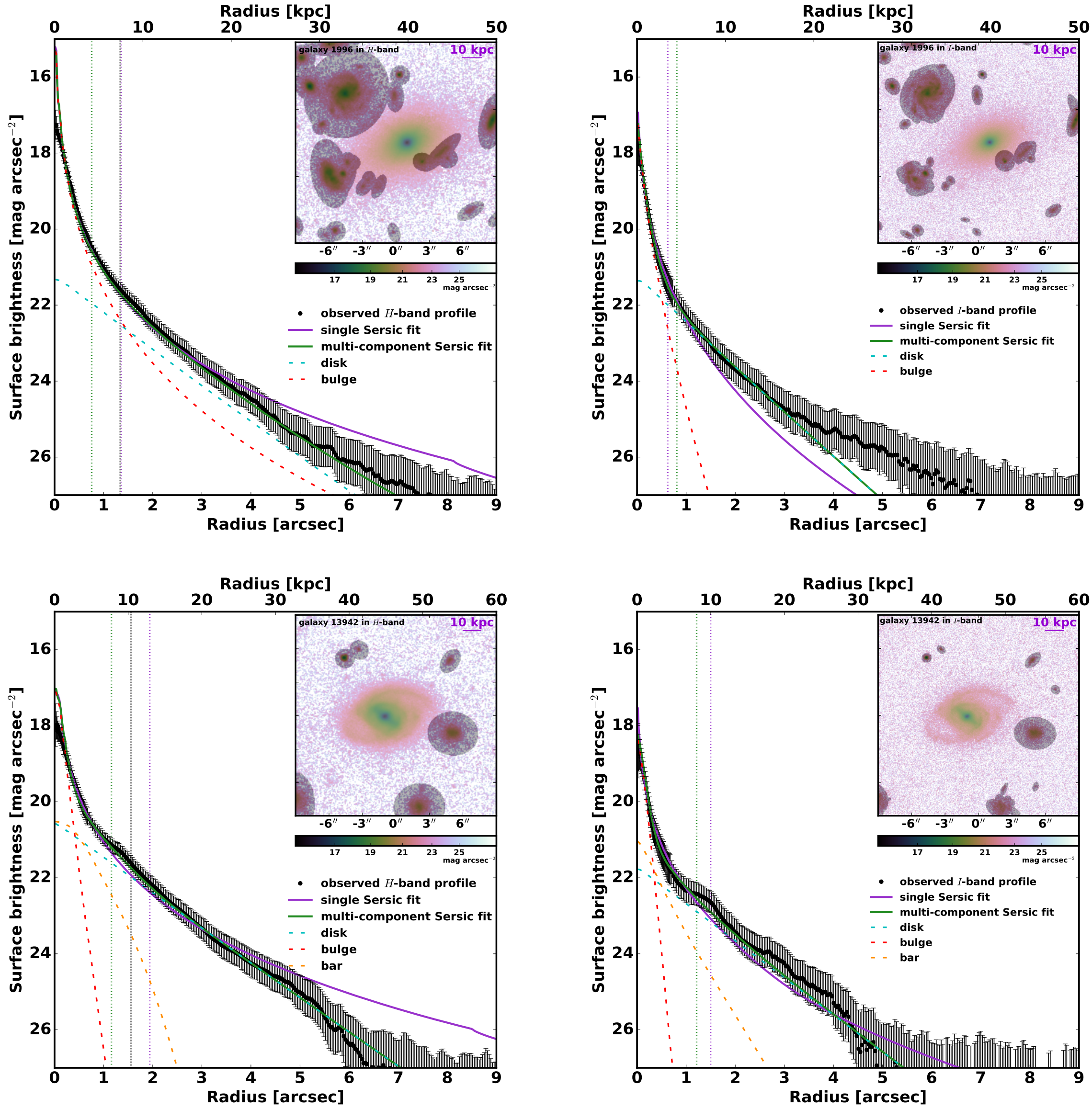

Figure 3: Surface brightness profiles in the H-band (left panels) and in the I-band (right panels) for two different morphological galaxies in our sample: ETG (top panels) and barred LTG (bottom panels). The violet and green colors correspond, respectively, to the results from single Sérsic fit and multi-component Sérsic fit. Black points represent the observed luminosity profile, solid lines show the models convolved with the PSF, dashed lines stand for the decomposition of the multi-component model into bulge (red), disk (blue) and bar (orange), dotted vertical lines represent the effective radius and the dotted grey vertical line is the [15] effective radius. We display the galaxy stamp in units of surface brightness (mag arcsec^{-2}) with shadowed areas matching the masks used to obtain the observed light profile, the galaxy ID on top left and a scale bar on top right corresponding to 10 kpc. The respective color bar is shown below the stamp.

Acknowledgments

This work was supported by FCT through national funds and by FEDER through COMPETE by the grants UID/FIS/04434/2013 & POCI-01-0145-FEDER-007672 and PTDC/FIS-AST/3214/2012 & FCOMP-01-0124-FEDER-029170. FB acknowledges the support by FCT via the postdoctoral fellowship SFRH/BPD/103958/2014. PP acknowledges support by FCT through Investigador FCT contract IF/01220/2013/CP1191/CT0002. This project has benefited from support by European Community Programme ([FP7/2007-2013]) under grant agreement No. PIRSES-GA-2013-612701 (SELGIFS). This work is based on observations taken by the CANDELS Multi-Cycle Treasury Program with the NASA/ESA HST, which is operated by the Association of Universities for Research in Astronomy, Inc., under NASA contract NAS5-26555.

References

[1] Bertin, E. & Arnouts, S. 1996, A&AS, 117, 393

[2] Bluck, A. F. L., Conselice, C. J., Buitrago, F., et al. 2012, ApJ, 747, 34

[3] Buitrago, F., Trujillo, I., Conselice, C. J., & Häußler, B. 2013, MNRAS, 428, 1460

[4] Ferreras, I., Hopkins, A. M., Gunawardhana, M. L. P., et al. 2017, MNRAS, 468, 607

[5] Ferreras, I., Trujillo, I., Mármol-Queraltó, E., et al. 2014, MNRAS, 444, 906

[6] Grogin, N. A., Kocevski, D. D., Faber, S. M., et al. 2011, ApJS, 197, 35

[7] Koekemoer, A. M., Faber, S. M., Ferguson, H. C., et al. 2011, ApJS, 197, 36

[8] López-Sanjuan, C., Balcells, M., Pérez-González, P. G., et al. 2010, ApJ, 710, 1170

[9] López-Sanjuan, C., Le Fèvre, O., de Ravel, L., et al. 2011, A&A, 530, A20

[10] López-Sanjuan, C., Le Fèvre, O., Ilbert, O., et al. 2012, A&A, 548, A7

[11] Mármol-Queraltó, E., Trujillo, I., Pérez-González, P. G., Varela, J., & Barro, G. 2012, MNRAS, 422, 2187

[12] Oser, L., Ostriker, J. P., Naab, T., Johansson, P. H., & Burkert, A. 2010, ApJ, 725, 2312

[13] Peng, C. Y., Ho, L. C., Impey, C. D., & Rix, H.-W. 2002, AJ, 124, 266

[14] Shen, S., Mo, H. J., White, S. D. M., et al. 2003, MNRAS, 343, 978

[15] van der Wel, A., Bell, E. F., Häußler, B., et al. 2012, ApJS, 203, 24

[16] van der Wel, A., Franx, M., van Dokkum, P. G., et al. 2014, ApJ, 788, 28